applied sciences

MDPI

Article

Root Cause Failure Analysis of Deep-Groove Ball Bearing Used in a Governor

Xueqin Hou [1,2,3,4,5,6,*], Yujian Liu [7], Tianyu Li [8], Changkui Liu [2,3,4,5,6], Zheng Zhang [1,*] and Chunhu Tao [2,3,4,5,6]

1 School of Material Science and Engineering, Beihang University, Beijing 100095, China
2 AECC Beijing Institute of Aeronautical Materials, Beijing 100095, China
3 Failure Analysis Center of Aviation Industry Corporation of China, Beijing 100095, China
4 Beijing Key Laboratory of Aeronautical Materials Testing and Evaluation, Beijing 100095, China
5 Aviation Key Laboratory of Science and Technology on Materials Testing and Evaluation, Beijing 100095, China
6 Key Laboratory of Science and Technology on Aeronautical Materials Testing and Evaluation, Aeroengine Corporation of China, Beijing 100095, China
7 AECC Harbin Bearing Co., Ltd., Harbin 150025, China
8 Huiyang Aviation Propeller Co., Ltd., Baoding 071051, China
* Correspondence: hxq001@buaa.edu.cn (X.H.); zhangzh@buaa.edu.cn (Z.Z.)

Abstract: Premature failure of a deep-groove ball bearing used in an aeroengine governor took place during service. In this paper, the failure mode and root cause of the bearing were studied by macroscopic and microscopic examination, metallographic analysis, hardness test, calculations of contact stress and L_{10} life, flatness measurement and comparative experiment. The results show that the failure modes of the inner ring raceway and steel balls are contact fatigue spalling, the failure modes of the outer ring raceway are wear and contact fatigue spalling, and the failure mode of the cage is fatigue fracture. The root cause and direct cause of the bearing failure were the unqualified machining process of the spring end face and the high unbalanced axial load, respectively. The unqualified machining process induced high points of the spring end face, which caused misalignment of the outer ring and inner ring and thereby resulted in the high unbalanced axial load. The characteristic damages induced by high axial load were climbing with the morphology of metal extrusion and accumulation at the border of the raceway for the inner and outer ring, and multiple fatigue fractures with the characteristic of multi origins for the cage. The unqualified machining process can be prevented by adopting the refined grinding process and adding detection requirements of flatness.

Keywords: root cause failure analysis; ball bearing; contact fatigue spalling; unbalanced load; unqualified machining

Citation: Hou, X.; Liu, Y.; Li, T.; Liu, C.; Zhang, Z.; Tao, C. Root Cause Failure Analysis of Deep-Groove Ball Bearing Used in a Governor. *Appl. Sci.* **2022**, *12*, 9658. https://doi.org/10.3390/app12199658

Academic Editor: Abílio Manuel Pinho de Jesus

Received: 14 August 2022
Accepted: 21 September 2022
Published: 26 September 2022

1. Introduction

Rolling element bearings are the basic components used to support the function of rotating parts and are extensively used in the engineering applications [1–4]. Under normal operating conditions, bearings will survive the expected life. However, with the high-pace improvement of products, high-quality requirements of bearings continually increase [5]. In addition, bearings are often subjected to a wide variety of severe operating conditions and harsh environments such as debris contamination, vibration and impact loading, which may result in pitting, flaking or spalling well before the bearings' rolling contact fatigue (RCF) design life [6,7].Therefore, bearing failures included the new unconventional bearing failure forms that have not been understood are often encountered [5].

Bearing failure leads to the failure of the rotating system, an increase in maintenance costs and time and a decrease in the safety applications, and has become one of the main causes of breakdown in rotating machinery [8]. In serious cases, it will lead to failure

of the whole machine or mechanical system, resulting in serious consequences such as air crashes [9]. Therefore, it is very important to master the failure modes and causes of bearings and then put forward countermeasures.

Bearing failure modes include spalling [10,11], fracture [12,13], wear [14], corrosion [15] and electric corrosion [16].The influencing factors causing each failure mode are relatively wide, including material microstructure, surface condition, assembly, lubrication, pollution, load and other factors. The root causes of bearing failures can be errors in design, manufacturing, assembly or operation [1,2,17,18]. Therefore, it is not easy to obtain the root cause of bearing failure, especially when the root cause of a bearing failure is a combination of several factors [7].

Meanwhile, bearing failure leaves traces of evidence (failure characteristics) on what caused its failure [19]. For example, enormous pitting damage to the bearing's ring raceway and rolling elements can be induced by excessive overloading [20]. Flaking on the raceways of the inner and outer rings of the bearing is a typical failure characteristic caused by excess tight assembly of the bearing [21,22]. Therefore, the cause of the bearing failure can be obtained by studying the failure characteristics of the bearing. It is also very important to master the relationship and manifestation between failure modes/characteristics and failure causes as much as possible for failure analysis and performance improvement of bearing.

Misalignment is one of the bearing failure causes and is often encountered in roller bearings, because—due to shaft bending, deflection of the bearing housing and inclination of rings induced by manufacturing or assembly errors—rollers frequently operate under a misaligned condition, which results in "eccentric load effect" (uneven contact pressure and stress distributions along the roller length) and thereby causes the unbalanced load failure of the bearing [23–25] Therefore, many people have studied the misalignment influence on bearings.

Qiu [26] proposed a new model that is capable of deterministically handling misalignment situations of cylindrical roller bearings and found that under the misalignment condition of the cylindrical roller bearing, significant pressure concentrations appear at the end of contact for all loaded rollers, and the pressure at the inner ring raceway is greater than that at the outer ring raceway, while the film thickness is the opposite. Li [27] studied the effect of misalignment error on contact pressure of the roller and found that the maximum contact pressure increased to about 3.7% when misalignment error of the bearing was 0.05°. Aditya [28] carried out failure analysis of a grease-lubricated cylindrical roller bearing and found that misalignments induced direct metal-to-metal contact between the cylindrical roller and inner ring raceway, then accelerated the wear rate of the cylindrical roller bearing. Savaskan [29] conducted an experimental study on the wear of a roller bearing and mentioned that the misalignment between the shaft and the bearing caused most of the wear of the bearing. Oktaviana [30] investigated the harmful effect of misalignment on the skidding of angular contact ball bearings by employing a five degrees-of-freedom quasi-static model and found that angular misalignment can introduce skidding areas in angular contact ball bearings preloaded by the constant force method, and the skidding does not increase, owing to angular misalignment when using the constant displacement preload method, because an additional axial load is induced.

From the above literature review, it can be concluded that most studies considered misalignment influence on bearings by numerical analysis. Little research has been performed in the investigation of ball bearing failure induced by misalignment. Failure modes and root causes of the bearing failure induced by misalignment need to be demonstrated.

Therefore, in this paper, the failure of a deep-groove ball bearing of a governor caused by misalignment is analyzed. The deep-groove ball bearing was found to prematurely fail during service after operation for 1400 h. The maximum axial load of the bearing was 128 N. The rotational speed of the bearing was 6400 rpm. The assembly structure of the failed deep-groove ball bearing is shown in Figure 1. The inner ring is assembled on the centrifugal block shaft and subjected to axial pressure from the centrifugal block shaft. The

outer ring is assembled on the bearing seat and supported by the axial pressure of the spring through spring housing. For the bearing, the axial pressure from the centrifugal block shaft and the axial pressure from the spring are a pair of balance forces.

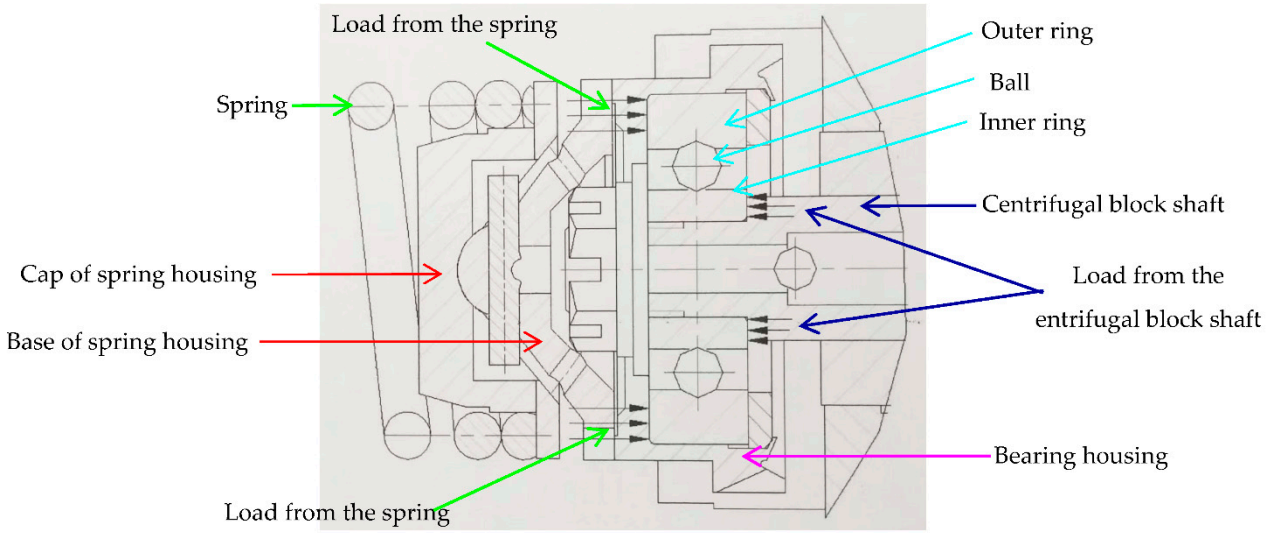

Figure 1. Assembly diagram of the deep-groove bearing.

Failure modes and root causes of the bearing failure are obtained by macroscopic and microscopic examination, metallographic analysis, hardness test, calculation of contact stress of the raceways and L_{10} life of the bearing, flatness measurement and comparative experiment. It is found that the failure mode of the inner ring raceway and steel balls is contact fatigue spalling, the failure mode of the cage is fatigue fracture, and the failure modes of the outer ring raceway are wear and contact fatigue spalling. The unqualified machining process was identified to be the root cause, leading to the greater flatness and high points in the spring end face, which induced misalignment of the bearing, thereby resulting in an unbalanced load on the bearing. This kind of fault can be prevented by adopting the refined grinding process and adding detection requirements of flatness.

2. Materials and Methods

Inner and outer rings and rolling elements of the bearing are made of ZGCr15 steel (equal to SAE 52100 and 100Cr6) with microstructures consisting of tempered martensite, primary spherical $(Fe,Cr)_3C$ and retained austenite. The amount of retained austenite is about5%. Chemical composition of ZGCr15 steel is shown in Table 1.

Table 1. Chemical compositions of ZGCr15 steel(wt.%).

Elements	C	Cr	Mn	Si	Cu	P	S
Content	1.03	1.56	0.37	0.29	0.16	0.021	0.006

Additionally, the cage is made of H62 brass with the microstructure composed of α and β phase. Chemical composition of H62 brass steel is shown in Table 2.

Table 2. Chemical compositions of H62 brass(wt.%).

Elements	Cu	Zn	Pb	Fe
Content	61.7	38.23	0.03	0.04

Macroscopic morphologies of the failure bearing were acquired by visual observation and examination with Leica DM6000stereo light microscope. Microscopic damage

morphologies of the bearing were examined by Camscan 3100 and Fei Nova nano SEM 450 scanning electron microscope. Microstructure of the bearing was examined by Olympus DM6000 optical metallographic microscope. The microhardness was measured by Q10A+ microhardness tester in the load of 1000 gf and dwell time of 15 s. Flatness of the spring end face was measured by three coordinate-measuring instruments. Contact fatigue test of the deep-groove bearing used for analysis verification of the root cause of the failure bearing was carried out in the governor test rig. And source of the above main experimental instruments used in in this paper are shown in Table 3.

Table 3. Main experimental instruments used in this paper.

Name	Type	Manufacturer
Stereo optical microscope	Leica DM6000	Leica Microsystems Inc., Wetzlar, Gernmany
Optical metallographic microscope	Olympus DM6000	Olympus Corporation, Tokyo, Japan
Scanning electron microscope	Camscan 3100	Obducat Camscan Ltd., Cambridge, United Kingdom
Scanning electron microscope	Fei Nova nano SEM 450	Thermo Fisher Scientific Inc., Brno, Czech Republic
Microhardness tester	Q10A+	QATM, Golling, Austria

3. Results

3.1. Macroscopic and Microscopic Observation

The deep-groove ball bearing is composed of an inner ring, an outer ring, a cage with two parts riveted and six steel balls. The appearance of the bearing and bearing housing disassembled from the governor is shown in Figure 2. One side of the cage is broken into three parts, and the other side of the cage has a fracture. The inner ring, outer ring, steel balls and bearing housing are damaged to different degrees, and the color of the bearing and bearing housing are normal.

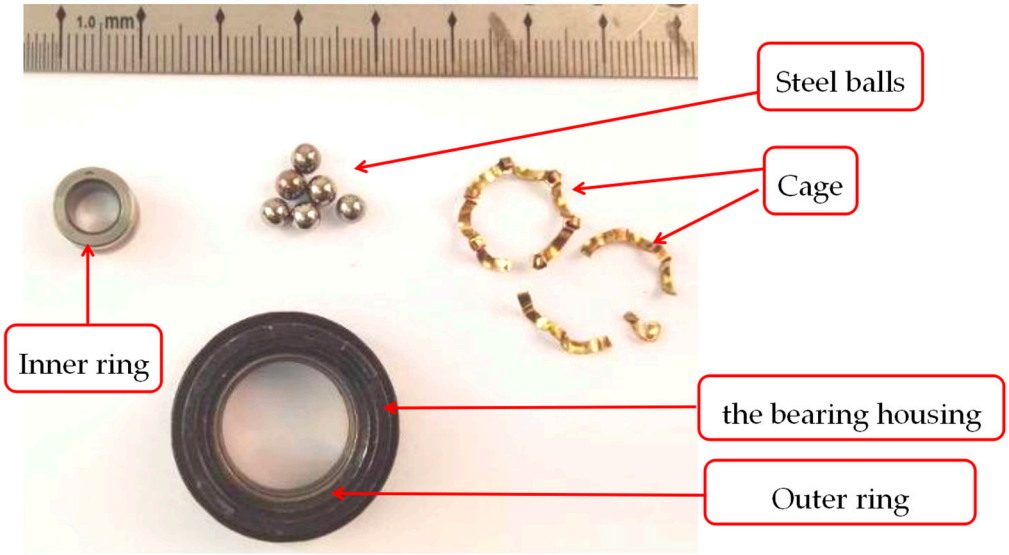

Figure 2. Appearance of the bearing and bearing housing.

The damage appearance of the inner ring raceway is shown in Figure 3. There is obvious spalling along the whole circumferential area adjacent to the centrifugal block shaft of the inner ring raceway. The damaged area can be roughly divided into three parts: the first part is the severely damaged area, which accounts for about 3/4 of the width of the inner ring raceway; the second part is the lightly damaged area, which accounts for about $\frac{1}{2}$ of the width of the inner ring raceway; and the third part is the least damaged area, which accounts for about $\frac{1}{2}$ of the width of the inner ring raceway and is located at the interface area between the severely damaged area and the lightly damaged area. There is metal

extrusion and accumulation at the border of the raceway near the side of the centrifugal block shaft.

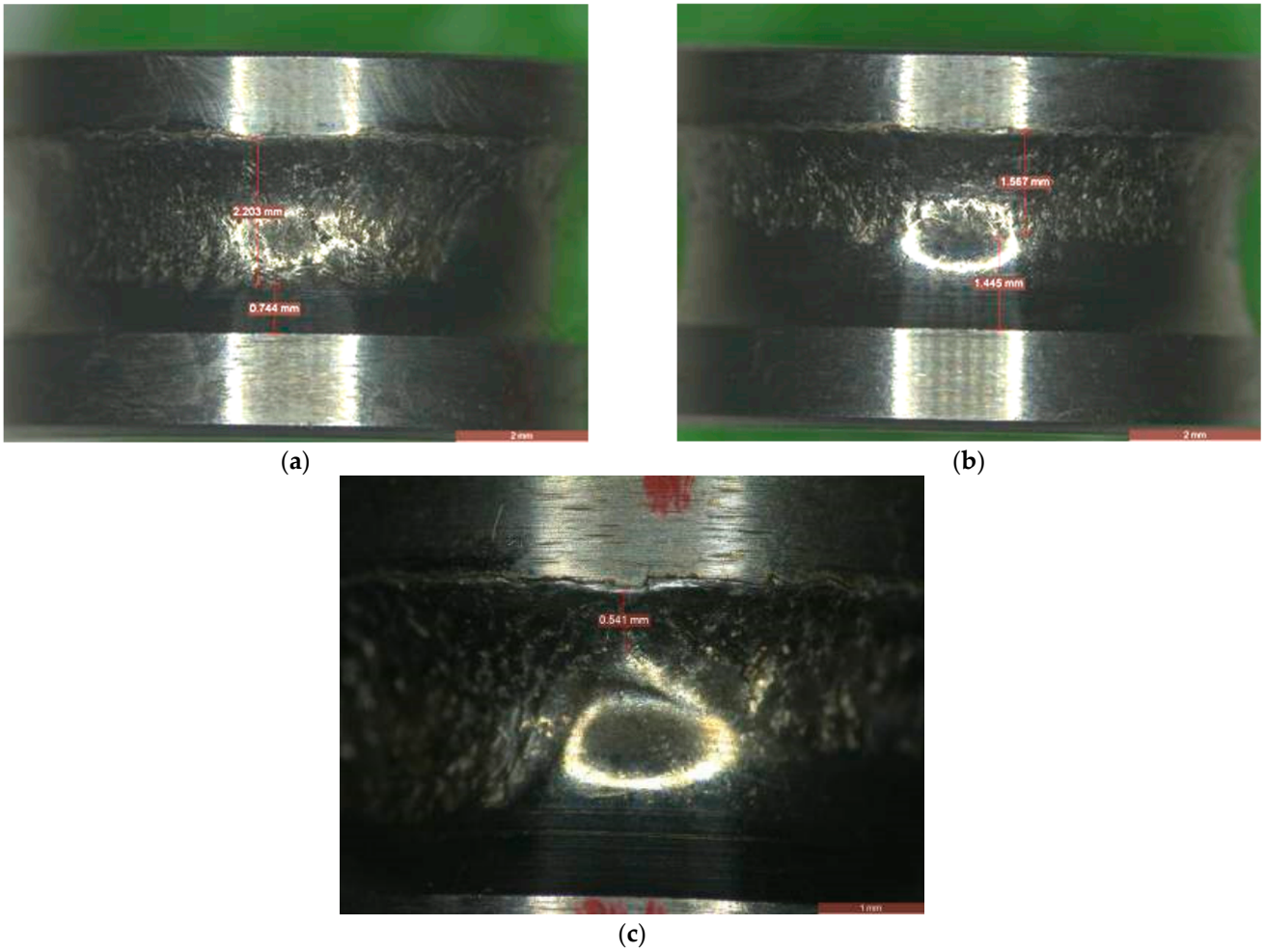

(**a**) (**b**)

(**c**)

Figure 3. Macroscopic damage of the inner ring raceway: (**a**) severely damaged area; (**b**) lightly damaged area; (**c**) least damaged area.

The spalling of the inner ring raceway is contact fatigue spalling characterized by pits and lamellar and chapped damage, as shown in Figure 4.

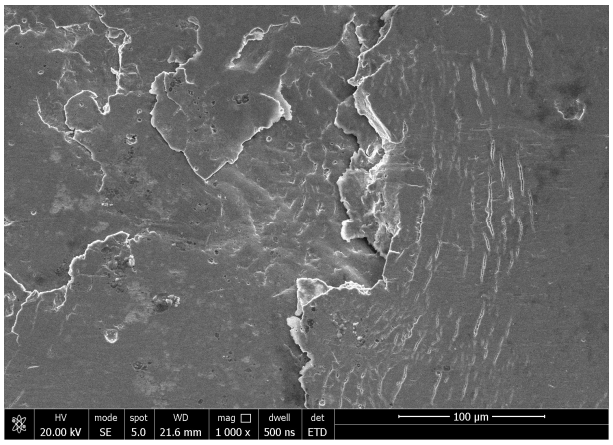

Figure 4. Contact fatigue spalling morphology of the inner ring raceway.

The typical microscopic morphology of metal extrusion and accumulation at the border of the raceway near the side of the centrifugal block shaft is shown in Figure 5.

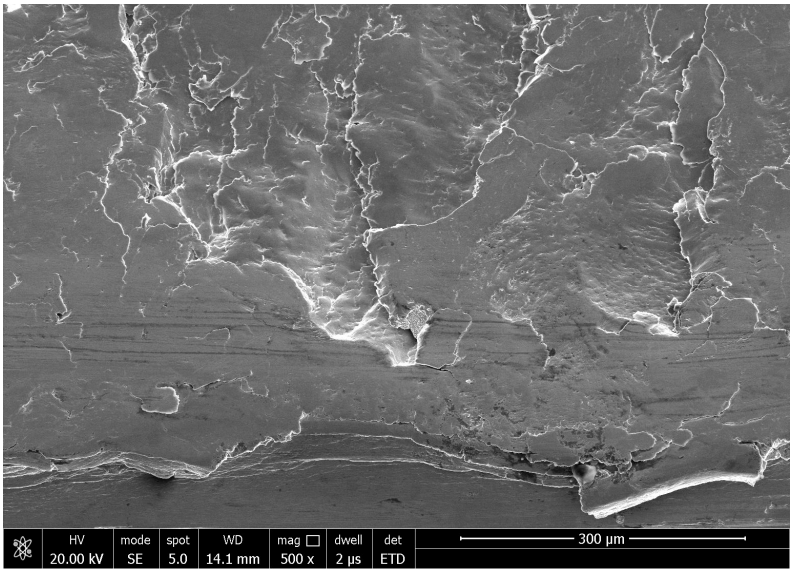

Figure 5. Metal extrusion and accumulation of the inner ring raceway.

According to the damage degree, the six steel balls can be roughly divided into two categories, namely heavily damaged balls, including four steel balls; and lightly damaged balls, including two steel balls. The heavily damaged steel balls mainly show contact fatigue spalling with characteristics of obvious fan-shaped morphologies, lamellar damage and cracks, as shown in the typical macroscopic and microscopic appearance in Figure 6a,b, respectively. The lightly damaged steel balls show light wear, as shown in the typical macroscopic and microscopic appearance in Figure 7a,b, respectively.

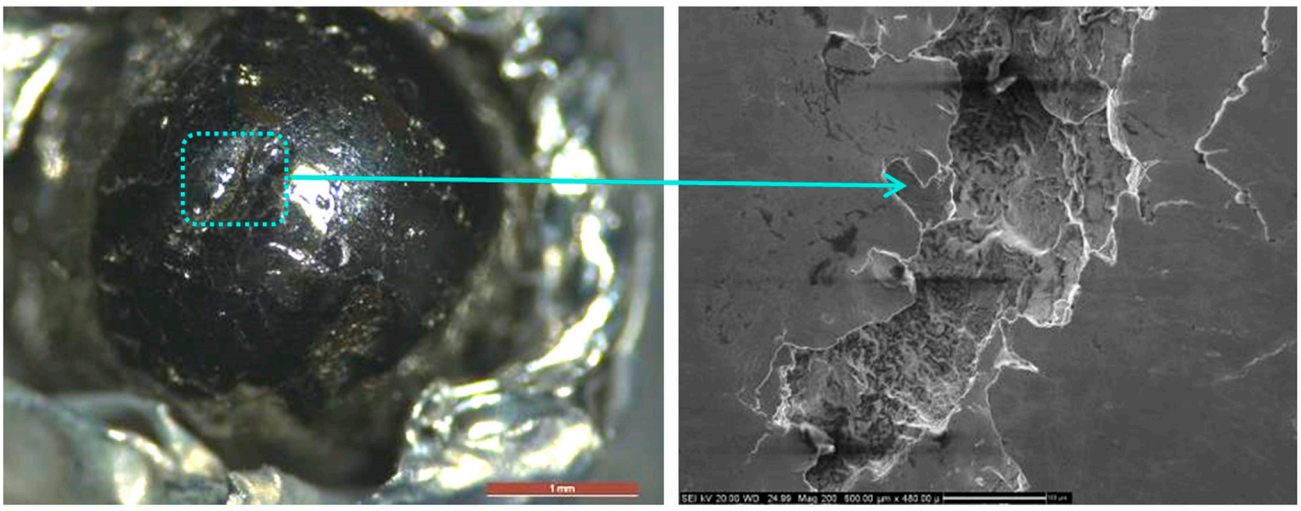

(**a**) (**b**)

Figure 6. Typical heavy damage appearance of the balls: (**a**) macroscopic appearance of contact fatigue spalling; (**b**) fan-shaped morphologies, lamellar damage and cracks.

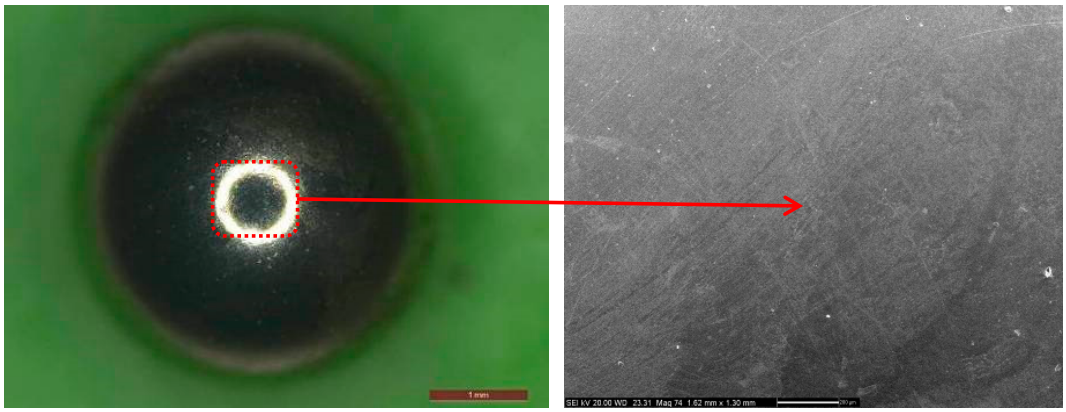

(**a**) (**b**)

Figure 7. Typical light damage appearance of the balls: (**a**) macroscopic appearance of the wear; (**b**) microscopic appearance of the wear.

The fracture surfaces of the cage are relatively flat without obvious plastic deformation. The fracture origins are located on the surface of the angle between two adjacent pockets. Fatigue striations can be seen in propagation areas of the fractures. The fractures of the cage are typical fatigue fractures with multi origins, as typically shown in Figure 8.

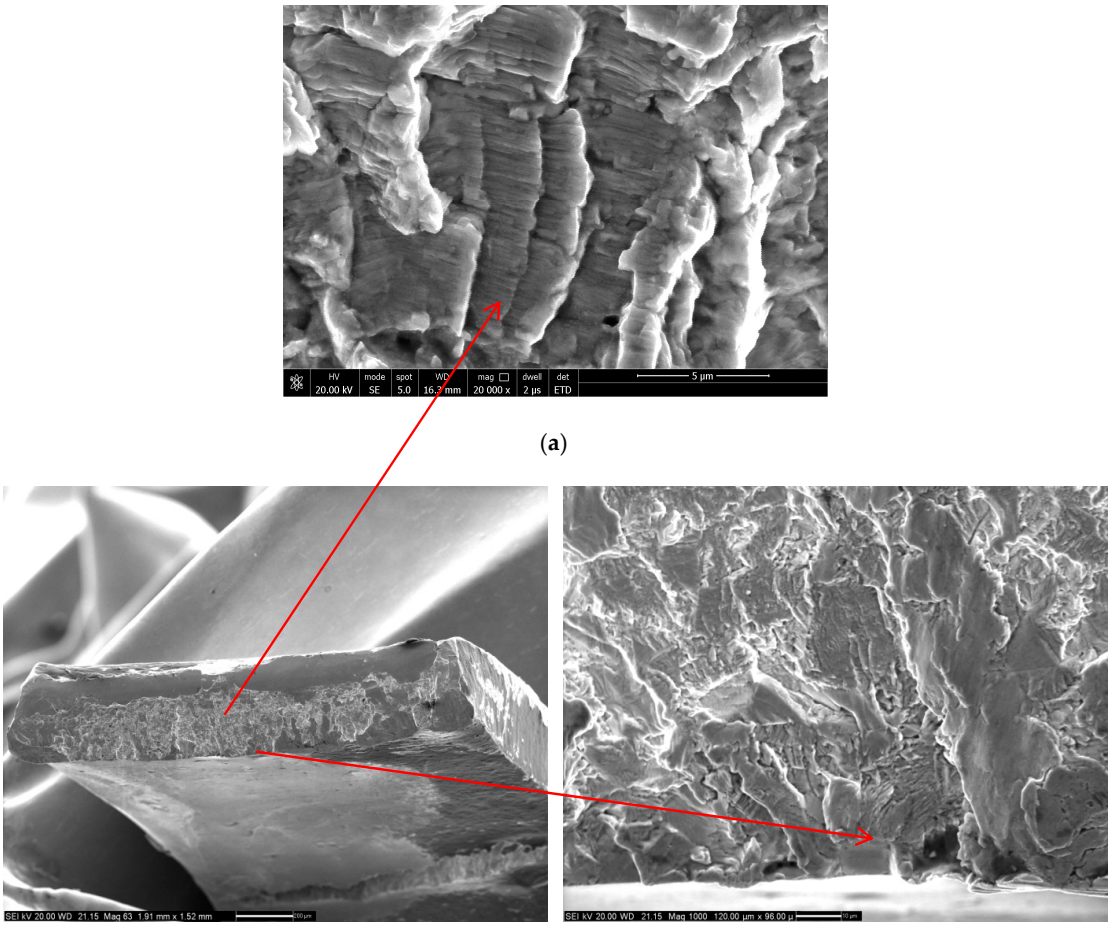

(**a**)

(**b**) (**c**)

Figure 8. Typical fracture morphology of the cage: (**a**) fatigue striations; (**b**) fracture appearance; (**c**) fracture origin.

The damage morphology of the outer ring raceway is an uneven-distribution circumferential wear strip located at the spring side with shallow wear, contact fatigue spalling and raceway surface metal squeezed to the guide surface, as shown in Figure 9.

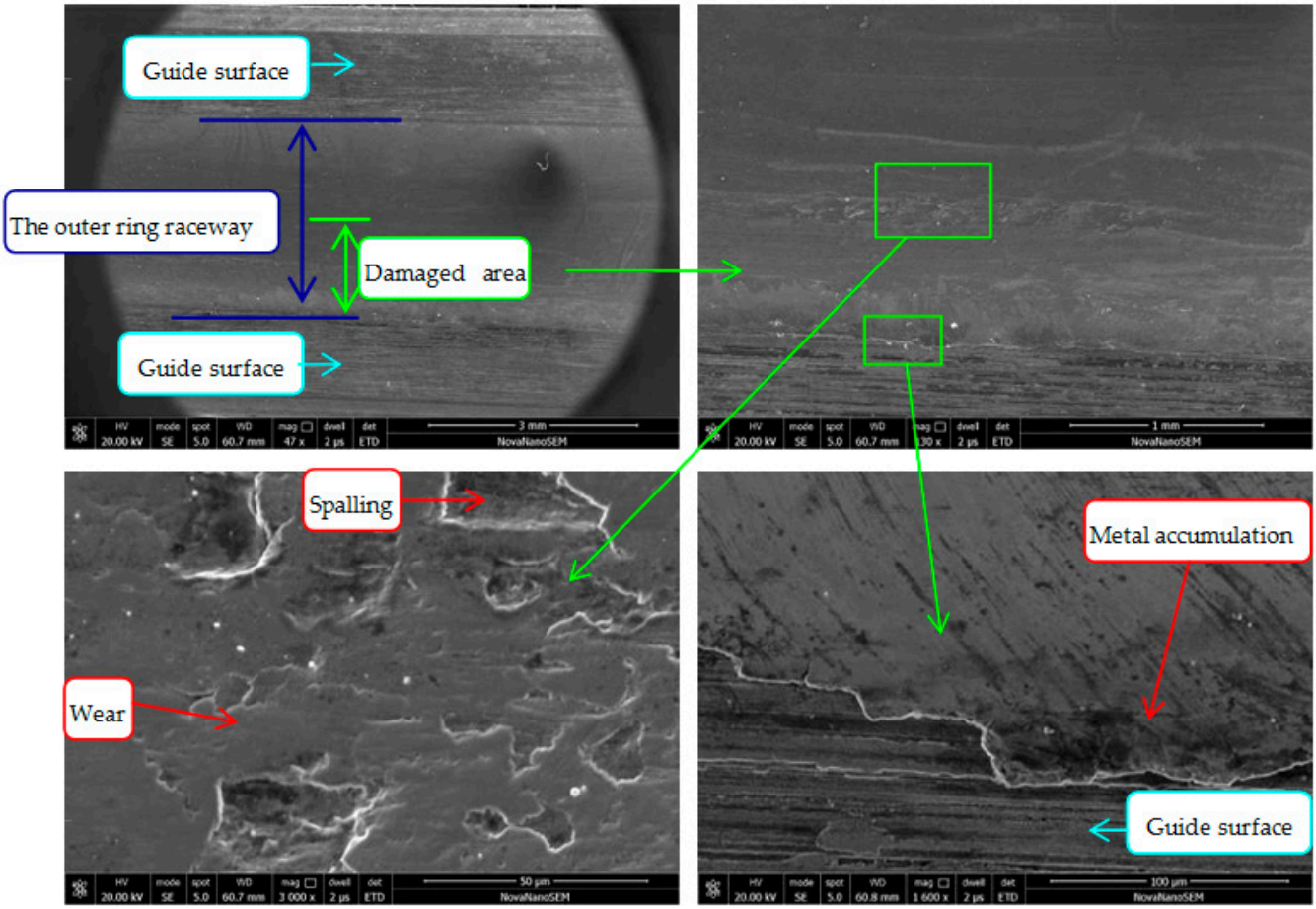

Figure 9. Damage morphology of the outer ring raceway.

3.2. Microstructure Examination

Metallographic samples were respectively taken from the heavily or lightly damaged areas of the inner ring, as shown in Figure 10. The microstructure of the inner ring is normal, characterized by tempered martensite and primary spherical $(Fe\ Cr)_3C$ carbide [31–33], while there are many cracks on the surface and subsurface of the inner ring raceway near the centrifugal block side. Raceway surface metal squeezed to the guide surface and deformation can also be seen at the centrifugal block side of the inner ring raceway.

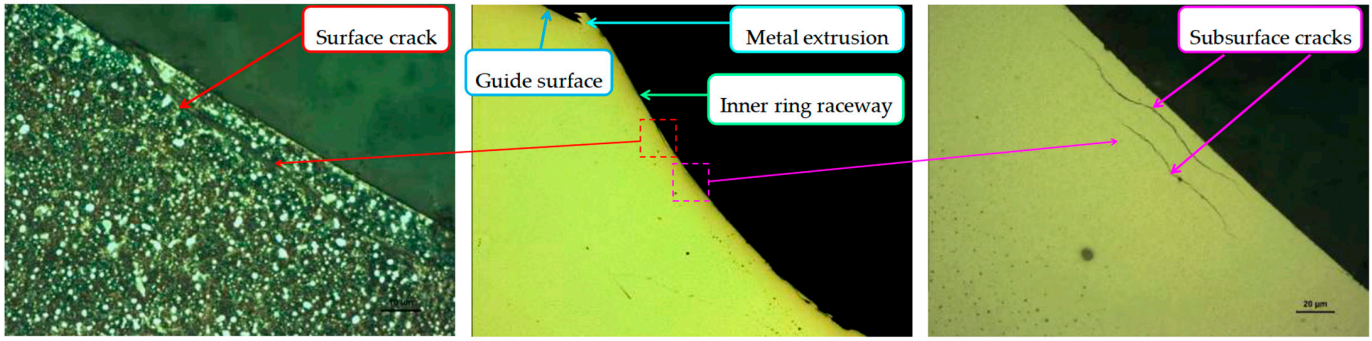

Figure 10. Microstructure, cracks and metal extrusion of the inner ring raceway.

Metallographic samples were taken from the outer ring, as shown in Figure 11. The microstructure of the outer ring is normal, characterized by tempered martensite and spherical $(Fe,Cr)_3$ C carbide. Raceway surface metal squeezed to the guide surface and deformation can also be seen at the spring side of the outer ring raceway.

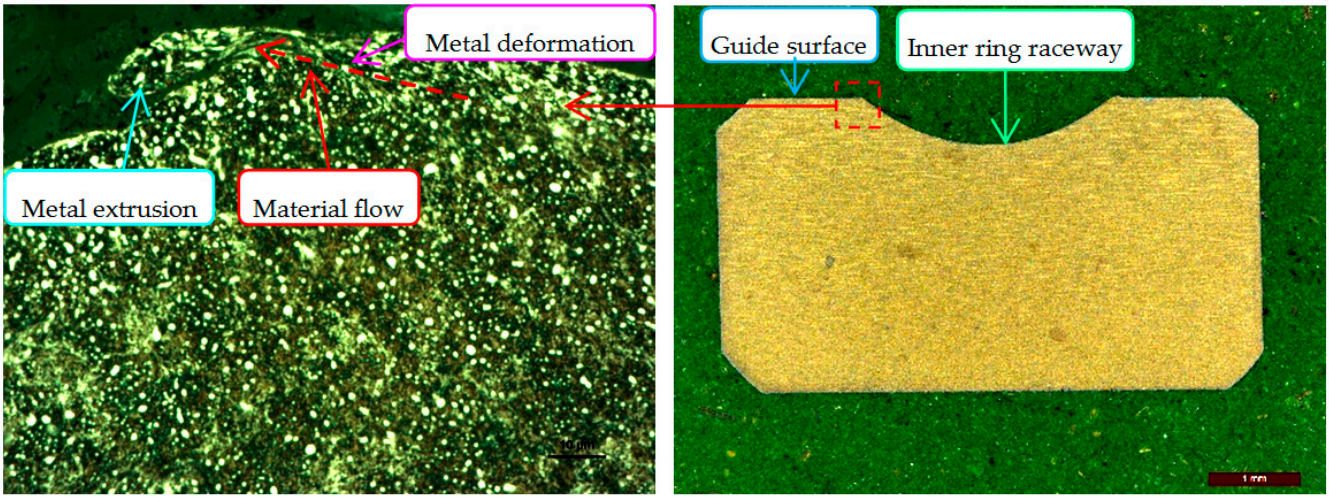

Figure 11. Microstructure, metal extrusion and deformation of the outer ring.

Metallographic samples were respectively taken from the heavily or lightly damaged steel balls. The microstructure of the steel balls is normal, characterized by tempered martensite and spherical $(Fe,Cr)_3$ C carbide, and there are many cracks on the surface layer of the severely damaged steel balls, as shown in Figure 12.

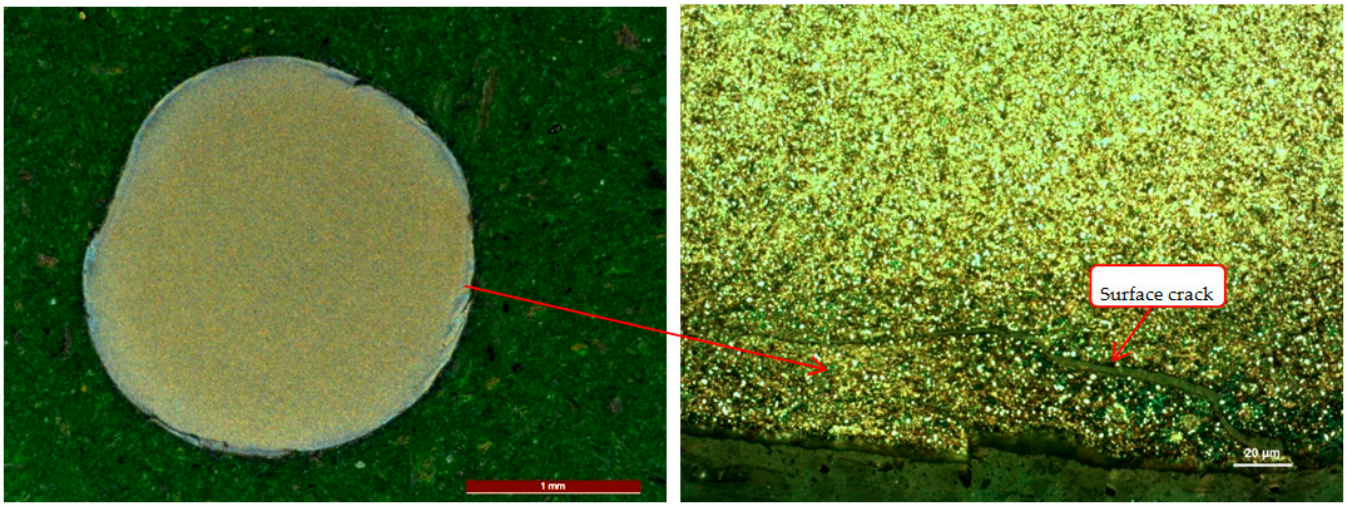

Figure 12. Microstructure and cracks of the heavily damaged ball.

The microstructure of the cage is normal and consists of an α and β phase [34], as shown in Figure 13. Cracks located on the surface of the angle between two adjacent pockets can be seen, as shown in Figure 14.

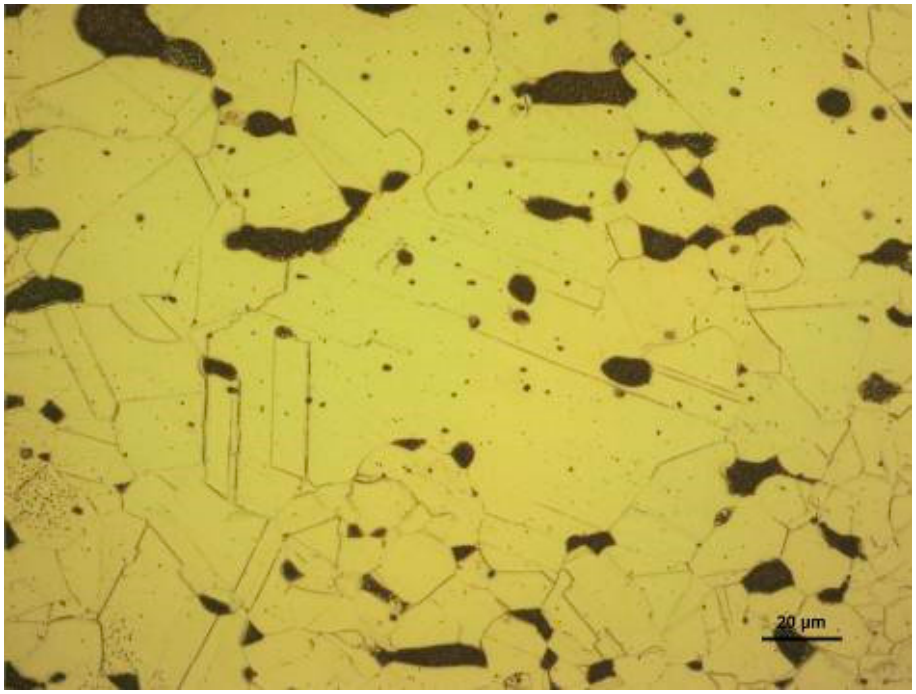

Figure 13. Microstructure of the cage.

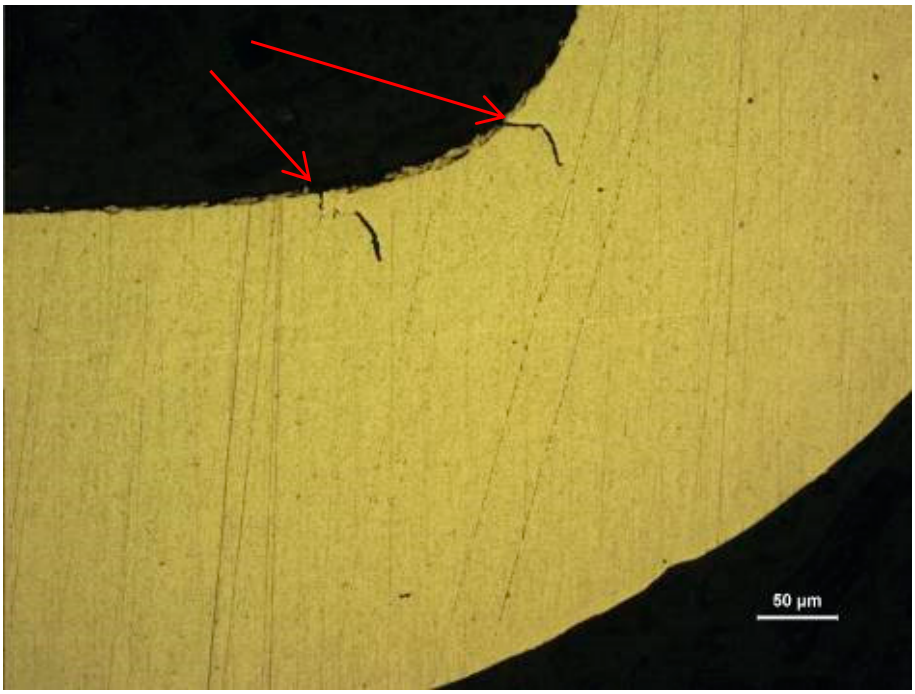

Figure 14. Cracks located on the angle of two adjacent pockets.

3.3. Hardness Examination

Hardness examination samples were respectively taken from the inner ring, outer ring and heavily or lightly damaged steel balls. The hardness requirements of the inner ring, outer ring and balls are HRC60.0 to HRC64.0. Their hardnesses are uniform, being HRC62.0, HRC62.5 and HRC63.0, separately.

4. Discussion

(1) Failure mode and direct failure cause

The failure mode of the inner ring raceway and steel balls is contact fatigue spalling. The failure modes of the outer ring raceway are wear and contact fatigue spalling. The failure mode of the cage is fatigue fracture.

Contact fatigue spalling and wear are the predominant modes of failure in rolling element bearings. They are affected not only by loading conditions but also by material properties, lubricants and surface conditions. Studies have shown that improper mounting, sealing and inadequate lubrication contribute to 90% of bearing failures [35,36]. There are no discoloration and overheating marks, according to the results of the damage appearance and microstructure examination results. Hence, failure of the bearing has nothing to do with insufficient lubrication [37,38]. The microstructures of the inner ring, outer ring raceway, steel balls and cage are normal. The hardness of the inner ring, outer ring raceway and steel balls meet the required specification. Therefore, the failure cause of the bearing is not related to the material quality, and the failure cause of the bearing should be high load.

The fact that the spalling damage area along the whole circumferential area adjacent to the centrifugal block shaft of the inner ring raceway can be roughly divided into three parts with different damage degrees indicates a high unbalanced load of the bearing. Moreover, the metal extrusion and accumulation at the border of the raceway near the side edge of the centrifugal block shaft indicates excessive axial load during the operation of the bearing [39]. Therefore, failure of the inner ring raceway should be related to a high unbalanced axial load of the bearing.

The damage morphology of the outer ring raceway is an uneven-distribution circumferential strip located at the spring side with shallow wear and spalling and raceway surface metals queezed to the guide surface. These characteristics indicate that a high unbalanced axial load may be the failure cause of the outer ring raceway.

One side of the cage is broken into three parts, and the other side of the cage has a fracture. This indicates that the side broken into three parts of the cage is subjected to a higher load than that of the other side, and the fatigue cause of the cage may be the high unbalanced axial load. Multi origins of the cage fatigue fractures indicate that the initial stress of the fracture was high and that the fracture should occur after the failure of the inner ring raceway, outer ring raceway and steel balls. There are two main reasons for the cage fracture: one is misalignment, and the other is an abnormal load acting on the cage in the bearing operation due to misaligned mounting between the inner and outer ring [40,41].Therefore, the high unbalanced axial load should be the cause of fatigue fracture of the cage.

The contact stress of the inner ring raceway and outer ring raceway of the deep-groove bearing were calculated by the ROMAX software, and the basic rating life (L_{10} life) on the contact fatigue of the deep-groove bearing was also calculated under different axial loads. The calculation results of the contact stress and L_{10} life are shown in Table 4. It can be seen that the contact stress increases with the increase in axial load and the L_{10} life decreases with the increase in axial load. Under the designed working conditions, the maximum axial load of the bearing is 128 N and has a L_{10} life of 2925 h, while the operation time of the failure groove ball bearing is 1440 h, which is smaller than 2925 h. In addition, the metal extrusion and accumulation at the border of the raceway indicate that the bearing was subjected to a large axial load during the failure process. Therefore, premature failure of the deep-groove ball bearing should be related to the high abnormal axial load.

Table 4. Calculation results of the contact stress and L_{10} life of the deep-groove bearing under different axial load.

Axial Load (N)	Contact Stress of the Inner Raceway (MPa)	Contact Stress of the Outer Raceway (MPa)	L_{10}Life (h)
115	1877	1426	3824
120	1898	1443	3442
128	1934	1470	2925
140	1983	1508	2312
150	2022	1538	1930
160	2059	1567	1637
180	2128	1620	1227
200	2191	1669	953

According to the above analysis results, the direct cause of the bearing failure should be the high unbalanced axial load, which may be induced by the misalignment of the bearing.

(2) Comprehensive analysis of the failure root cause

Load on the bearing is a pair of balancing forces acting on the inner ring and outer ring, respectively, by the centrifugal block shaft and spring, whose load is applied on the outer ring by the spring housing and spring base. Because the inner ring is fixed on the centrifugal block shaft with good positioning, the high unbalanced axial loadis not caused by the centrifugal block shaft. Therefore, the high unbalanced axial load may be caused by the spring, spring housing or spring base.

There are two contact marks on the end face of the spring, which match the two marks on the corresponding spring housing, as shown in Figure 15. The spring and the spring housing are not in whole surface contact as required by the design, but in local contact. The centers of the spring and the cap are not on the connecting line between their two marks. This will induce misalignment of the outer ring and inner ring and thereby induce a high unbalanced axial load, as shown in Figure 16.

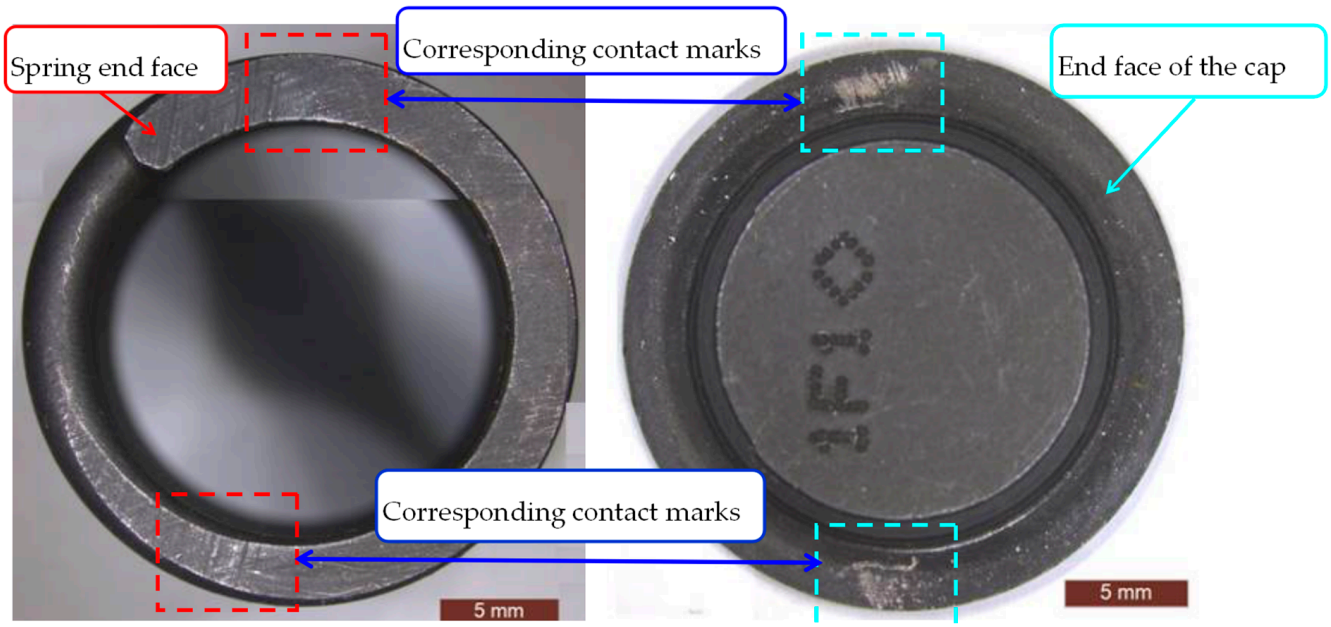

Figure 15. Two contact marks in the end face of the spring and the cap.

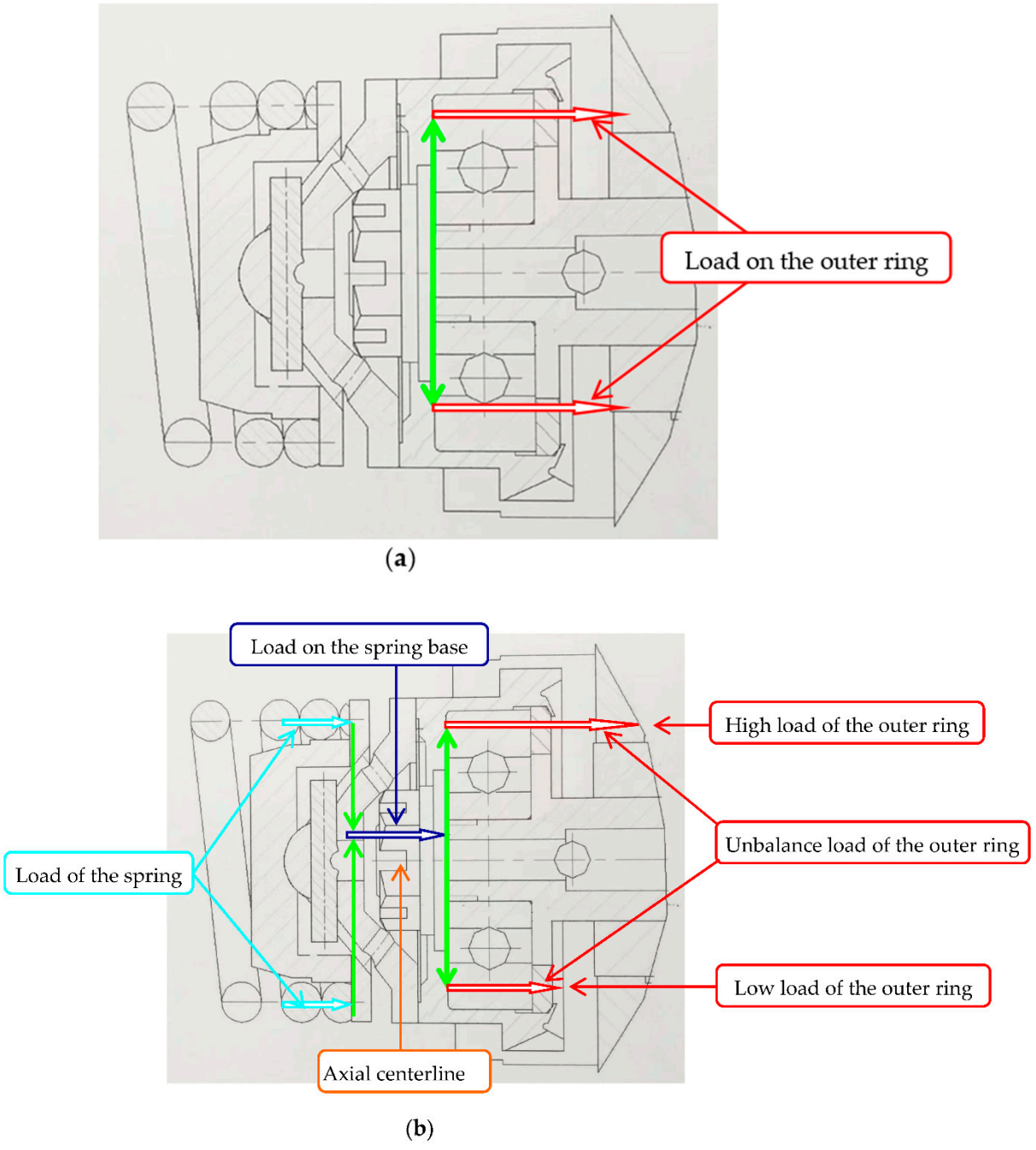

Figure 16. Transmission path of spring force received by outer ring: (**a**) under the normal condition of whole surface contact; (**b**) under the abnormal condition of local contact.

The flatness examination result of the cap end face is normal, while the flatness examination result of the spring end face is 0.2, which is greater than 0.1 of the technical requirement. It is also found that the end face of the spring is composed of two planes, with one plane being large and the other plane being small. Therefore, high points are formed by the intersection of the two planes in areas of the above two contact marks.

(3) Comparative experiment

In order to determine the influence of greater flatness and high points in the spring end face on working state of the deep-groove ball bearing, a comparative experiment was carried out on the spring (faulty spring)corresponding to the failure bearing. The faulty spring with a new deep-groove bearing was installed in the governor and assembled on the

test equipment. The comparative experimental parameters were adopted from the normal working conditions of the governor.

After testing for 50 h, the damage morphology of the corresponding bearing was acquired by visual observation and stereo light microscope examination and the damage morphology of the test bearing was compared with that of the failure bearing, and that of the bearing corresponded to the normal spring which was normally worked for 1400 h.

Working tracks of the outer ring raceway of the test bearing and failure bearing were almost the same. Their working tracks intersected with the guide surface, resulting in a certain degree of climbing, metal extrusion and accumulation at the spring side border of the raceway, which originated from the raceway and propagated to the guide surface, as shown in Figure 17a,b. Meanwhile, for the bearing corresponding to the normal spring, there was a certain distance between the working track of the outer ring raceway and the guide surface, and no climbing phenomenon, as shown in Figure 17c. Therefore, it can be concluded that the high axial load on the bearing was induced by high points of the faulty spring end face, and the unbalanced load caused the bearing failure during service.

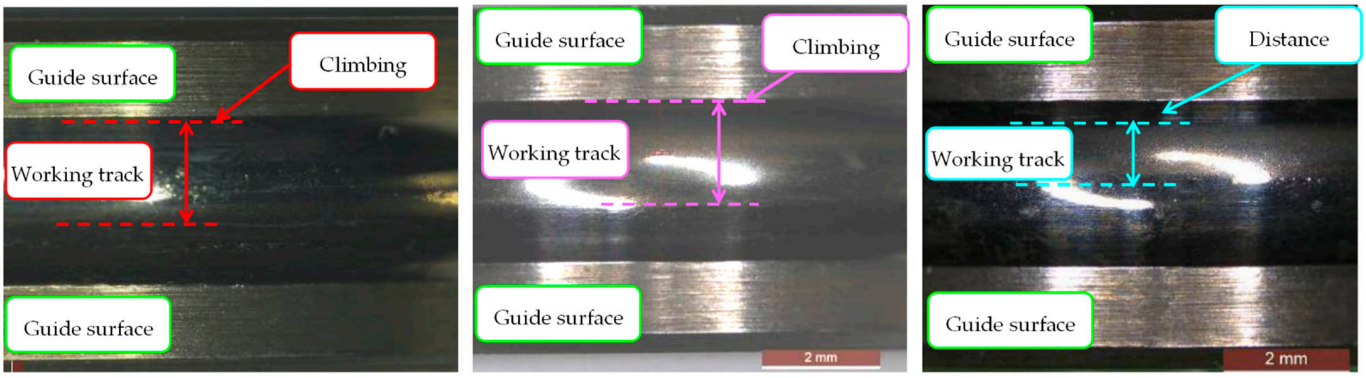

(**a**) (**b**) (**c**)

Figure 17. Comparison of the working tracks.(**a**)Working track of the outer ring raceway of the failure bearing; (**b**)working track of the outer ring raceway of the test bearing corresponding to the faulty spring; (**c**)working track of the outer ring raceway of the bearing corresponding to the normal spring.

Through the examination of the spring processing, it is found that greater flatness and high points of the spring end face are induced by improper processing and can be prevented by adopting a refined grinding process and adding detection requirements of flatness.

5. Conclusions

A deep-groove ball bearing was found to prematurely fail during service after operation for 1400 h.Failure analysis of the deep-groove ball bearing was carried out. Based on the observation of macroscopic and microscopic damage morphologies, the failure mode of the failed bearing was analyzed. The direct and root causes of the bearing failure were investigated by tests such as examinations of microstructure and hardness, calculations of contact stress and L_{10} life, and flatness measurement, as well as a comparative experiment. Several results were arrived to, and are shown as follows:

(1) The failure mode of the inner ring raceway and steel balls is contact fatigue spalling. The failure modes of the outer ring raceway are wear and contact fatigue spalling. The failure mode of the cage is fatigue fracture.

(2) Both the inner ring raceway and outer ring raceway exhibited the high axial load-induced damage characteristic of climbing with the morphology of metal extrusion and accumulation at the border of the raceway. The cage exhibited multiple fatigue fractures, with the characteristic of multi origins under the effect of high unbalanced axial load.

(3) The direct cause of the bearing failure is the high unbalanced axial load. The root cause of the bearing failure is the unqualified machining process of the spring end face. High points of the spring end face caused by the unqualified machining process induced misalignment of the outer ring and inner ring, and thereby caused the high unbalanced axial load.
(4) The high points can be prevented by adopting the refined grinding process and adding detection requirements of flatness.

Author Contributions: Conceptualization, X.H. and Z.Z.; methodology, X.H.; validation, X.H. and Y.L.; formal analysis, X.H.; investigation, X.H. and T.L.; resources, X.H. and Y.L.; data curation, Z.Z., C.L. and C.T.; writing—original draft preparation, X.H.; writing—review and editing, Z.Z. and T.L.; supervision, Z.Z., C.L. and C.T.; project administration, C.L.; funding acquisition, C.L. All authors have read and agreed to the published version of the manuscript.

Funding: This research was funded by the Independent Innovation Foundation of Aero Engine Corporation of China, grant number ZZCX-2018-026.

Institutional Review Board Statement: Not applicable.

Informed Consent Statement: Not applicable.

Data Availability Statement: Not applicable.

Acknowledgments: The authors are grateful to senior engineer Guoping Li for his technical support and materials used for experiments.

Conflicts of Interest: The authors declare no conflict of interest.

References

1. Kudelina, K.; Baraškova, T.; Shirokova, V.; Vaimann, T.; Rassõlkin, A. Fault detecting accuracy of mechanical damages in rolling bearings. *Machines* **2022**, *10*, 86. [CrossRef]
2. Hong, S.; Tong, V. Rolling-element bearing modeling: A review. *Int. J. Precis. Eng. Manuf.* **2016**, *17*, 1729–1749. [CrossRef]
3. Kishore, K.; Mukhopadhyay, G. Root cause failure analysis of pinch roll bearing at Hot Strip Mill. *J. Fail. Anal. Preven.* **2019**, *19*, 219–229. [CrossRef]
4. Bakoglidis, K.D.; Nedelcu, I.; Ivanov, I.G.; Meeuwenoord, R.; Schmidt, S.; Janzén, E.; Ehret, P.; Greczynski, G.; Hultman, L. Rolling performance of carbon nitride-coated bearing components in different lubrication regimes. *Tribol. Int.* **2017**, *114*, 141–151. [CrossRef]
5. Alhasia, S.; Gindy, S.; Arslan, S.; Jawad, B.; Riedel, C. Analysis of failure modes of bearing outer race rotation. *SAE Int. J. Passeng. Cars-Electron. Electr. Syst.* **2015**, *8*, 240–243. [CrossRef]
6. Gould, B.; Greco, A.; Stadler, K.; Vegter, E.; Xiao, X. Using advanced tomography techniques to investigate the development of White Etching Cracks in a prematurely failed field bearing. *Tribol. Int.* **2017**, *116*, 362–370. [CrossRef]
7. Murugesan, V.; Sreejith, P.S.; Sundaresan, P.B.; Ramasubramanian, V. Analysis of an angular contact ball bearing failure and strategies for failure prevention. *J. Fail. Anal. Prev.* **2018**, *18*, 471–485. [CrossRef]
8. Cong, F.; Chen, J.; Dong, G.; Petcht, M. Vibration model of rolling element bearings in a rotor bearing system for fault diagnosis. *J. Sound Vib.* **2013**, *332*, 2081–2097. [CrossRef]
9. Salam, I.; Tauqir, A.; Haq, A.U.; Khany, A.Q. An air crash due to fatigue failure of a ball bearing. *Eng. Fail. Anal.* **1998**, *5*, 261–269. [CrossRef]
10. Gloeckner, P.; Sebald, W.; Bakolas, V. An approach to understanding micro-spalling in high-speed ball bearings using a thermal elastohydrodynamic model. *Tribol. Trans.* **2019**, *52*, 534–543. [CrossRef]
11. Walvekar, A.A.; Paulson, N.; Farshid, S.; Nick, W.; Martin, C. A new approach for fatigue damage modeling of subsurface-initiated spalling in large rolling contacts. *J. Tribol.* **2017**, *139*, 011101. [CrossRef]
12. Yu, Z.; Yang, Z. Failure analysis of fatigue fracture on the outer ring of a cylindrical roller bearing in an air blower motor. *J. Fail. Anal. Preven.* **2012**, *12*, 427–437. [CrossRef]
13. Xu, L.; Yu, Z. Failure analysis of tapered roller bearing inner rings used in heavy truck. *Eng. Fail. Anal.* **2020**, *111*, 104474. [CrossRef]
14. Gagg, C.R.; Lewis, P.R. Wear as a product failure mechanism—Overview and case studies. *Eng. Fail. Anal.* **2007**, *14*, 1618–1640. [CrossRef]
15. Magalhaes, J.F.; Ventsel, L.; Macdonald, D.D. Environmental effects on pitting corrosion of AISI440C ball bearing steels—experimental results. *J. Soc. Tribol. Lubr. Eng.* **1999**, *55*, 36–41.
16. Prashad, H. Diagnosis of rolling-element bearings failure by localized electrical current between track surfaces of races and rolling-elements. *J. Tribol. Trans. ASME* **2002**, *124*, 468–473. [CrossRef]

17. Manieri, F.; Stadler, K.; Morales-Espejel, G.E.; Kadiric, A. The origins of white etching cracks and their significance to rolling bearing failures. *Int. J. Fatigue* **2019**, *120*, 107–133. [CrossRef]
18. Errichello, R.; Budny, R.; Eckert, R. Investigations of bearing failures associated with White Etching Areas (WEAs) in wind turbine gearboxes. *Tribol. Trans.* **2013**, *56*, 1069–1076. [CrossRef]
19. Vartha, V.; Kumar, A.; Saxon, M.; Rajan, A.; John, B.; Tharian, T.; Cherian, S. Failure analysis of ball-bearing of turbo-pump used in liquid rocket engine. *Mater. Sci. Forum* **2015**, *830–831*, 709–712. [CrossRef]
20. Juliš, M.; Čelko, L.; Spotz, Z.; Doležal, P.; Pavloušková, Z.; Švejcar, J. Failure analysis of spherical roller bearing. *Mater. Sci. Forum* **2014**, *782*, 247–250. [CrossRef]
21. Mishra, R.; Muduli, S.; Srinivasan, K.; Ahmed, S. Failure Analysis of an Inter-shaft Bearing of an Aero Gas Turbine Engine. *J Fail. Anal. Preven.* **2015**, *15*, 205–210. [CrossRef]
22. Harris, T.A.; Barnsby, R.M. Tribological performance prediction of aircraft gas turbine main shaft ball bearings. *Tribol. Trans.* **1998**, *41*, 60–68. [CrossRef]
23. Fan, G.; Yu, Q.; Gong, P.; Liu, X.; Yan, G. Analysis and improvement of cylindrical roller bearing failure. *Fail. Anal. Prev.* **2021**, *16*, 129–133.
24. Xue, B.; Chen, S.; Ren, Y.; Yin, F.; Shan, T.; Shao, M. Effect of tempering heat treatment on microstructure and mechanical properties of GCr15 bearing steel. *J. Shandong Univ. Technol.* **2021**, *35*, 73–76.
25. Warda, B.; Chudzik, A. Effect of ring misalignment on the fatigue life of the radial cylindrical roller bearing. *Int. J. Mech. Sci.* **2016**, *111–112*, 1–11. [CrossRef]
26. Qiu, L.; Liu, S.; Chen, X.; Wang, Z. Lubrication and loading characteristics of cylindrical roller bearings with misalignment and roller modifications. *Tribol. Int.* **2022**, *165*, 107291. [CrossRef]
27. Li, S. Strength analysis of the roller bearing with a crowning and misalignment error. *Eng. Fail. Anal.* **2021**, *123*, 105311. [CrossRef]
28. Aditya, S.; Amarnath, M.; Kankar, P. Failure analysis of a grease-lubricated cylindrical roller bearing. *Procedia Technol.* **2014**, *14*, 59–66. [CrossRef]
29. Savaskan, T. On the wear and failure of high speed roller bearings. *Wear* **1987**, *116*, 361–380. [CrossRef]
30. Oktaviana, L.; Tong, V.; Hong, S. Skidding analysis of angular contact ball bearing subjected to radial load and angular misalignment. *J. Mech. Sci. Technol.* **2019**, *33*, 837–845. [CrossRef]
31. Wang, G. Effect of Tempering Temperature on Microstructure and Properties of GCr15 Bearing Steel. *Fail. Anal. Prev.* **2016**, *11*, 361–363.
32. Smelova, V.; Schwedt, A.; Wang, L.; Holweger, W.; Mayer, J. Electron microscopy investigations of microstructural alterations due to classical rolling contact fatigue(RCF) in martensitic AISI 52100 bearing steel. *Int. J. Fatigue* **2017**, *98*, 142–154. [CrossRef]
33. Warhadpande, A.; Sadeghi, F.; Evans, R.D. Microstructural alterations in bearing steels under rolling contact fatigue part 1: Historical overview. *Tribol. Trans.* **2013**, *56*, 349–358. [CrossRef]
34. Jin, Y.; Zeng, X.; Sun, Z.; Zhou, D.; Cui, Y. Analysis of punching-induced crack of H62 brass washer. *Heat Treat. Met.* **2016**, *41*, 197–200.
35. Harris, T.A.; Kotzalas, M.N. *Advanced Concepts of Bearing Technology: Rolling Bearing Analysis*, 5th ed.; CRC Press: Boca Raton, FL, USA, 2016; p. 235.
36. Laithy, M.E.; Wang, L.; Harvey, T.J.; Vierneusel, B.; Correns, M.; Blass, T. Further understanding of rolling contact fatigue in rolling element bearings—A review. *Tribol. Int.* **2019**, *140*, 105849. [CrossRef]
37. Halme, J.; Anderson, P. Rolling contact fatigue and wear fundamentals for rolling bearing diagnostics-state of the art. *Proc. Inst. Mech. Eng. Part J* **2009**, *224*, 377–393. [CrossRef]
38. John, S.; Mishra, R.; Hari, K.; Ramesha, H.; Ram, K. Investigation of bearing failure in a turbo shaft engine. *J. Fail. Anal. Preven.* **2020**, *20*, 34–39. [CrossRef]
39. Ejaz, N.; Ali, L.; Rizvi, S. Failure of an aero engine ball bearing due to axial loading. *J. Fail. Anal. Preven.* **2015**, *15*, 15–24. [CrossRef]
40. *ISO 15243: 2017*; Rolling Bearings—Damage and Failures–Terms, Characteristics and Causes. International Organization for Standardization: Geneva, Switzerland, 2017.
41. Wang, P.; Yang, Y.; Ma, H.; Xu, H.; Li, X.; Luo, Z.; Wen, B. Vibration characteristics of rotor-bearing system with angular misalignment and cage fracture: Simulation and experiment. *Mech. Syst. Signal Process.* **2023**, *182*, 109545. [CrossRef]